NANO LETTERS

Letter

pubs.acs.org/NanoLett

Theory of Half-Space Light Absorption Enhancement for Leaky Mode Resonant Nanowires

Yiming Jia,[†] Min Qiu,[‡] Hui Wu,[§] Yi Cui,[∥] Shanhui Fan,[⊥] and Zhichao Ruan*,[†]

[†]State Key Laboratory of Modern Optical Instrumentation and Department of Physics, Zhejiang University, Hangzhou 310027, China

[‡]State Key Laboratory of Modern Optical Instrumentation and Department of Optical Engineering, Zhejiang University, Hangzhou 310027, China

[§]State Key Laboratory of New Ceramics and Fine Processing, School of Materials Science and Engineering, Tsinghua University, Beijing 100084, China

[∥]Department of Materials Science and Engineering, Stanford University, Stanford, California 94305, United States

[⊥]Department of Electrical Engineering and Ginzton Laboratory, Stanford University, Stanford, California 94305, United States

ABSTRACT: Semiconductor nanowires supporting leaky mode resonances have been used to increase light absorption in optoelectronic applications from solar cell to photodetector and sensor. The light conventionally illuminates these devices with a wide range of different incident angles from half space. Currently, most of the investigated nanowires have centrosymmetric geometry cross section, such as circle, hexagon, and rectangle. Here we show that the absorption capability of these symmetrical nanowires has an upper limit under the half-space illumination. Based on the temporal coupled-mode equation, we develop a reciprocity theory for leaky mode resonances in order to connect the angle-dependent absorption cross section and the radiation pattern. We show that in order to exceed such a half-space limit the radiation pattern should be noncentrosymmetric and dominate in the direction reciprocal to the illumination. As an example, we design a metal trough structure to achieve the desired radiation pattern for an embedded nanowire. In comparison to a single nanowire case the trough structure indeed overcomes the half-space limit and leads to 39% and 64% absorption enhancement in TM and TE polarizations, respectively. Also the trough structure enables the enhancement over a broad wavelength range.

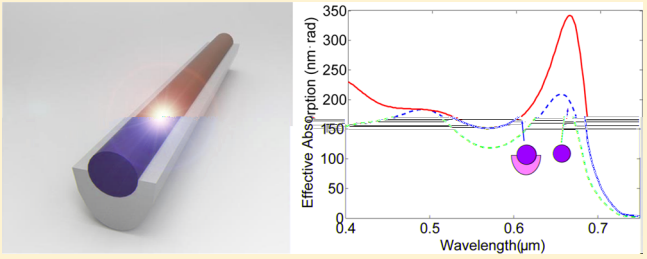

KEYWORDS: *Nanowire, absorption, solar cell, photodetector, coupled-mode theory, leaky mode resonance*

Semiconductor nanowires have been explored extensively over the past decades due to their potential applications in high-performance optoelectronic devices, including photodetectors,[1−10] solar cells,[11−22] and sensors.[23−27] The small size of nanowires provides opportunities for further miniaturization of these devices, which will lead to many advantages in terms of operation performance, signal-to-noise ratio, and power generation. However, due to the diffraction limit, the miniaturized devices cannot capture enough incident photons and result in unsatisfactory external quantum efficiency. Recently, it has been demonstrated that leaky mode resonances (LMRs) in nanowires can efficiently enhance light absorption.[1] The resonant absorption enhancement has been successfully used in photodetectors[1,2] and solar cells.[11,12] Cao et al. demonstrated that LMRs effectively enhance the external quantum efficiency of Ge nanowire photodetectors especially at the important 1.55 μm communication wavelength.[2] The LMRs have also been utilized to increase absorption efficiency of solar cell, and about 25% increase in short circuit current has been observed as compared with the planar structure.[12] A core-shell nanowire, which supports several nearly degenerate LMRs, has been demonstrated to lead to enhanced absorption in an a-Si shell.[11]

We note that in the applications of solar cells and photodetectors, nanowires typically operate in the configuration where light illuminates the nanowire with a wide range of different incident angles from half space (Figure 1a). Currently, most of the geometric cross sections of the investigated nanowires have centrosymmetry, such as circle,[2,11,12,16] hexagon,[12,22] and rectangle.[12,28] However, we recently have shown that for nanowires supporting a single LMR, the integration of the absorption cross section over all angles, $\int_0^{2\pi} C_{abs}(\phi)\, d\phi$ has a maximum of λ, where λ is the light wavelength in free space and ϕ is the incident angle.[29] For the nanowires with centrosymmetry, the incident-angle dependent absorption cross section satisfies $C_{abs}(\phi) = C_{abs}(\phi + \pi)$. Therefore, the absorption cross section integrated over half space has an upper limit of $\lambda/2$ (i.e., the incident angle ϕ from

Received: May 25, 2015
Revised: July 14, 2015
Published: July 14, 2015

DOI: 10.1021/acs.nanolett.5b02044
Nano Lett. 2015, 15, 5513−5518

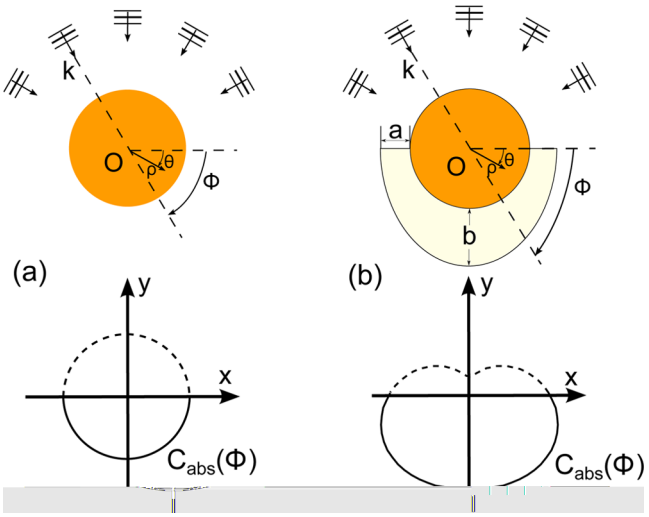

Figure 1. (a) Schematic of the half-space light absorption limit for nanowires, which have centrosymmetric geometry cross sections. For nanowires supporting a single LMR, the integration of the absorption cross section over all angles, $\int_0^{2\pi} C_{abs}(\phi)\ d\phi$ has a maximum of λ, where λ is the light wavelength in free space and ϕ is the incident angle. Due to the centrosymmetry of the nanowire, it has $C_{abs}(\phi) = C_{abs}(\phi + \pi)$. Therefore, when the light illuminates the structures from half space, e.g., the incident angle ϕ ranging from 0 to π, the absorption cross section integrated over half space has an upper limit of $\lambda/2$. (ρ,θ) is the polar coordinates. (b) Schematic of the half-space light absorption enhancement by breaking the centrosymmetry. The wire-trough structure consists of an a-Si nanowire and a silver trough. The trough has a half-elliptical outer boundary. The thickness of the through along the short and long axes is a and b, respectively.

0 to π as illustrated in Figure 1a), which here we refer to as *half-space limit*.

In this Letter, based on the temporal coupled-mode theory (CMT) formalism,[29−32] we develop a reciprocity theory for LMR nanowires. We show that the incident-angle dependent absorption cross section is determined by the radiation pattern of LMR. In order to exceed the half-space limit the radiation pattern of leaky mode resonances should be noncentrosymmetric and dominate in the directions that are reciprocal to the directions of illumination. As an example, we design a metal trough structure to achieve the desired radiation pattern for an embedded nanowire. As a result, the trough structure indeed overcomes the half-space limit in comparison to the case of a single nanowire. The integration of the absorption cross sections for the half-space illumination is enhanced by 39% and 64% as compared with a half-space limit single nanowire, in TM and TE polarization, respectively. Moreover, we also show that the structure enables the enhancement over a broad wavelength range.

We first develop the reciprocity theory based on the temporal coupled-mode equation. Here we consider that a TM polarized plane wave, which has its magnetic field normal to the nanowire axis and its electric field only in the axial direction, is incident on the nanowire located at the origin. Similar derivation can be carried out for the TE polarized case, which has its electric field normal to the nanowire axis. For the TM polarization, the total electric field for the far-field can be written as

$$E_{total}(\rho, \theta) = A_0 \frac{\exp(-ik\rho)}{\sqrt{\rho}} |a^+(\theta)\rangle + A_0 \frac{\exp(ik\rho)}{\sqrt{\rho}} |a^-(\theta)\rangle \tag{1}$$

where (ρ,θ) is the polar coordinates, k is the wave vector in the free space, and A_0 is a normalization coefficient. We take the convention that the field varies in time as $\exp(-i\omega t)$. So $|a^+\rangle$ and $|a^-\rangle$ can be identified as the incoming and outgoing wave amplitudes, respectively. With the choice of $A_0 = \left(\frac{4\mu_0}{\varepsilon_0}\right)^{1/4}$, $\langle a^+|a^+\rangle$ and $\langle a^-|a^-\rangle$ represent the time-averaged power of the incoming and outgoing waves.[30,31] Here $\langle f|g\rangle$ denotes the integration $\int_0^{2\pi} f^*(\theta) g(\theta)\ d\theta$ over all angles.

When the nanowire supports a single LMR, the far field of the resonant mode can be written as

$$E_{LMR}(\rho, \theta) = A_0 \frac{\exp(ik\rho)}{\sqrt{\rho}} |d(\theta)\rangle \tag{2}$$

where the function $|d(\theta)\rangle$ represents the radiation pattern of the LMR. In this case, the scattering process can be described by the temporal coupled-mode theory with the equations:[29,30,32]

$$\frac{dc}{dt} = (-i\omega_0 - \gamma - \gamma_0)c + \langle d^*|a^+\rangle \tag{3a}$$

$$|a^-\rangle = \hat{B}|a^+\rangle + c|d\rangle \tag{3b}$$

where c is the amplitude of the resonance, ω_0 is the resonant frequency, γ_0 is the intrinsic loss rate due to absorption in the nanowire, γ is the external leakage rate due to the coupling of the resonance to the outgoing wave, $\hat{B}$ is the scattering operator for a background scattering process that is independent of the resonance, and $\hat{B}^\dagger\hat{B} = 1$. The amplitude c is normalized such that $|c|^2$ corresponds to the energy inside the nanowire.

According to the temporal coupled-mode theory,[29,30,32] $|d\rangle$ and $\hat{B}$ are constraint due to the energy conversation and time-reversal symmetry, as a result

$$\langle d|d\rangle = 2\gamma \tag{4a}$$

$$\hat{B}|d^*\rangle = -|d\rangle \tag{4b}$$

Now we define a scattering operator that connects the incoming and the outgoing wave: $|a^-\rangle = \hat{S}|a^+\rangle$. From the temporal coupled-mode theory eq 3, we have

$$\hat{S} = \hat{B} + \frac{|d\rangle\langle d^*|}{i(\omega_0 - \omega) + \gamma + \gamma_0} \tag{5}$$

To evaluate the absorption cross section, we suppose a TM polarized incident plane wave $E_{inc} = \exp(i\mathbf{k}\cdot\mathbf{r})$. The absorbed power by the nanowire:

$$P_{abs} = \langle a^+|a^+\rangle - \langle a^-|a^-\rangle = \langle a^+|(1 - \hat{S}^\dagger\hat{S})|a^+\rangle \tag{6}$$

Substituting eq 5 into eq 6, we can obtain the absorption cross section as

$$C_{abs} = \frac{P_{abs}}{I} = \sqrt{\frac{\mu_0}{\varepsilon_0}} \frac{4\gamma_0}{(\omega - \omega_0)^2 + (\gamma + \gamma_0)^2} |\langle d^*|a^+\rangle|^2 \tag{7}$$

DOI: 10.1021/acs.nanolett.5b02044
Nano Lett. 2015, 15, 5513−5518

where $I = \frac{1}{2}\sqrt{\frac{\varepsilon_0}{\mu_0}}$ is the incident power. Equation 7 shows that generally the absorption cross section of a LMR nanowire exhibits a Lorentzian line shape around the resonant frequency.

To obtain the incident-angle dependence of the absorption cross section, we now expand the plane wave into cylindrical waves as

$$\exp(i\mathbf{k}\cdot\mathbf{r}) = \sum_{m=-\infty}^{\infty} i^m \exp(-im\phi)\left(\frac{H_m^{(1)}(k\rho) + H_m^{(2)}(k\rho)}{2}\right) \times \exp(im\theta) \quad (8)$$

where ϕ is the incident angle of the plane wave illustrated in Figure 1a. In the far field, where $k\rho \to \infty$, eq 8 can be rewritten as

$$\begin{aligned}\exp(i\mathbf{k}\cdot\mathbf{r}) &\approx \frac{\exp(ik\rho)}{\sqrt{\rho}}\sqrt{\frac{1}{2\pi k}}\exp\left(-\frac{i\pi}{4}\right)\sum_{m=-\infty}^{\infty}\exp[im(\theta-\phi)] + \frac{\exp(-ik\rho)}{\sqrt{\rho}}\sqrt{\frac{1}{2\pi k}}\exp\left(\frac{i\pi}{4}\right)\sum_{m=-\infty}^{\infty}\exp[im(\theta-\phi-\pi)]\\ &= \frac{\exp(ik\rho)}{\sqrt{\rho}}\sqrt{\frac{2\pi}{k}}\exp\left(-\frac{i\pi}{4}\right)\delta(\theta-\phi) + \frac{\exp(-ik\rho)}{\sqrt{\rho}}\sqrt{\frac{2\pi}{k}}\exp\left(\frac{i\pi}{4}\right)\delta[\theta-(\phi+\pi)]\end{aligned} \quad (9)$$

where δ is the Dirac delta function, and we utilize the equation $\delta(\theta) = \frac{1}{2\pi}\sum_{m=-\infty}^{\infty}\exp(im\theta)$. By comparing eq 9 with eq 1, we then have

$$|a^+\rangle = \sqrt{\frac{\pi}{\omega\mu_0}}\exp\left(i\frac{\pi}{4}\right)\delta[\theta-(\phi+\pi)] \quad (10)$$

Substituting eq 10 into eq 7, we get the incident-angle dependent absorption cross section:

$$C_{abs}(\phi) = \lambda\frac{2\gamma_0}{(\omega-\omega_0)^2 + (\gamma+\gamma_0)^2}|d(\phi+\pi)|^2 \quad (11)$$

eq 11 outlines the general reciprocity relation between the incident-angle dependent absorption of nanowires and the radiation pattern of the leaky resonant mode. As eq 11 shows, the incident-angle dependent absorption cross section is proportional to the radiation pattern of the LMR in the direction reciprocal to the illumination, i.e., $C_{abs}(\phi) \propto |d(\phi+\pi)|^2$. By integrating the absorption cross section over all angles and substituting eq 11, we have

$$\begin{aligned}\int_0^{2\pi} C_{abs}(\phi)\,d\phi &= \lambda\frac{2\gamma_0}{(\omega-\omega_0)^2+(\gamma+\gamma_0)^2}\langle d|d\rangle\\ &= 4\lambda\frac{\gamma_0\gamma}{(\omega-\omega_0)^2+(\gamma+\gamma_0)^2}\end{aligned} \quad (12)$$

eq 12 shows that the integration of absorption cross sections over all angles has a maximum of λ at the resonant frequency, when the resonance reaches the critical coupling, i.e., $\gamma = \gamma_0$. We note that for the nanowires with centrosymmetric geometry cross section, the radiation pattern also has centrosymmetry, i.e., $|d(\theta+\pi)|^2 = |d(\theta)|^2$. Therefore, the integration of absorption cross section over half space (i.e., the incident angle ϕ from 0 to π as illustrated in Figure 1a) always has the upper limit of $\lambda/2$.

In order to make the half-space absorption exceed the limit, we need to break the centrosymmetry in the nanowire geometry and design the structure with a noncentrosymmetric radiation pattern of LMR. Equation 11 shows that a desired radiation pattern of LMR should dominate in the direction reciprocal to illumination: When the incident angle ranges from $\phi = 0$ to $\phi = \pi$, it requires to suppress the radiation of LMR mode in the direction from $\theta = 0$ to $\theta = \pi$. Moreover, due to a wide range of different incident angles, the lobe of the radiation pattern should dominate from $\theta = \pi$ to $\theta = 2\pi$.

We note that nanowire structures may support doubly degenerate or nearly degenerate resonances, e.g., TM_{ml} mode in nanowires when the angle momentum index $m \neq 0$. In this case, if two LMRs are orthogonal, i.e., $\langle d_1|d_2\rangle = 0$, the total absorption cross section is a sum of the contributions from the two resonances:

$$C_{total}(\phi) = \lambda\left(\frac{2\gamma_{01}}{(\omega-\omega_{01})^2+(\gamma_1+\gamma_{01})^2}|d_1(\theta+\pi)|^2 + \frac{2\gamma_{02}}{(\omega-\omega_{02})^2+(\gamma_2+\gamma_{02})^2}|d_2(\theta+\pi)|^2\right) \quad (13)$$

where ω_{0i}, γ_i, γ_{0i}, and $|d_i(\theta)\rangle$ $(i = 1,2)$ correspond to the resonant frequency, the external leaky rate, the intrinsic loss rate, and the radiation pattern of the two LMRs, respectively. In the case of doubly degenerate LMRs, the integration of the total absorption cross section over all angles has a maximum of 2λ. For a nanowire having centrosymmetry that supports a pair of degenerate LMRs, the radiation pattern $|d_i(\theta)\rangle$ may not have the full symmetry of the structure. However, the radiation pattern of each degenerate mode still has centrosymmetry, i.e., $|d_i(\theta+\pi)|^2 = |d_i(\theta)|^2$. Correspondingly, there is still an upper limit of λ for the total absorption cross section under half-space light. Therefore, in order to exceed such a limit, we need to break the centrosymmetry of the nanowire geometry even though the nanowire supports degenerate resonances.

Now we demonstrate the half-space absorption enhancement by breaking the centrosymmetric geometry with a wire-trough structure (Figure 1b). We have recently fabricated such a metal trough with standard evaporation technique, and experimentally demonstrated that a metallic trough network is a remarkable transparent electrode with great mechanical flexibility.[33] Here we show that the trough structure can be used to control the radiation of LMR and enhance the light absorption of embedded nanowire for a wide range of different incident angles from half space.

To show the half-space absorption enhancement, we compare the wire-trough structure to a single nanorod with a circular geometric cross section. According to C. Garnet's study, a single a-Si nanorod has the optimal absorptive performance for the solar spectrum when the nanorod has a diameter around 110 nm. Such a rod has two degenerate TM_{11} resonances reaching the critical coupling at 654 nm wavelength.[11] Here we use a commercial finite element method (FEM) software (COMSOL) to design a silver trough structure and assume that the trough has a half-elliptical outer boundary (Figure 1b). The frequency-dependent dielectric constants of a-Si and silver are taken from the experiments.[34] The silver

DOI: 10.1021/acs.nanolett.5b02044
Nano Lett. 2015, 15, 5513−5518

trough is characterized by two thicknesses a and b, as shown in Figure 1b. To realize LMRs resonating in the vicinity of 650 nm, we first set $a = b = 30$ nm and modify the diameter of the embedded nanowire while keeping the wire and the trough touching. Our simulation shows that an embedded nanowire with a 125 nm diameter supports two nearly degenerate TM_{11} resonances at 658 nm (Figure 2a). According to the mirror

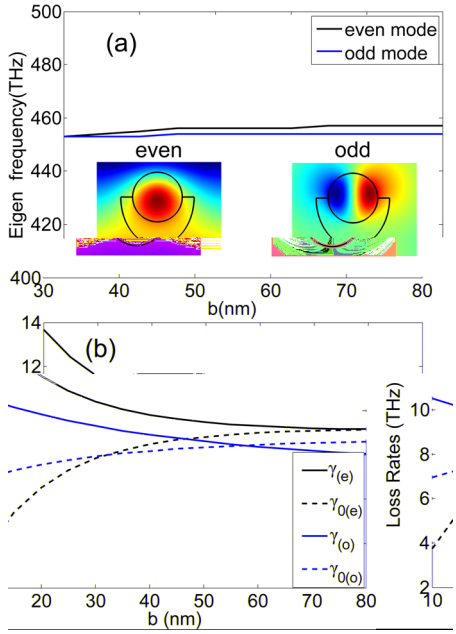

Figure 2. (a) Resonant frequency of the even and odd LMRs in the wire-trough structure, schematically shown in Figure 1b. The inset shows the electric field distribution of two modes. (b) The external leaky rate $\gamma_{(e,o)}$ and the intrinsic loss rate $\gamma_{0(e,o)}$ of the even and the odd LMRs vary as a function of b, where the thickness $a = 30$ nm.

symmetry around the y-axis of the wire-trough structure, the two TM_{11} resonances can be classified into an even and an odd mode (the inset in Figure 2a). In order to maximize the absorption cross section, we need to ensure that the two LMRs are not only degenerate but also working close to the critical coupling, i.e., $\gamma_0 = \gamma$. For this purpose, we fix $a = 30$ nm and modify b. Figure 2b plots that γ and γ_0 of both resonances vary as functions of b. Here we choose $b = 60$ nm, and in this case the two LMRs are nearly critically coupled.

Next we show that the trough structure allows a desired radiation pattern to enhance the half-space absorption. We plot the radiation patterns for both resonances in Figure 3a at the wavelength of 658 nm. Especially it shows that the radiation pattern of the even LMR dominates in the angles from $\theta = \pi$ to $\theta = 2\pi$, which is distinct from the single nanorod. Such a modification is attributed to the trough structure, which is nearly a perfect electric conductor for the TM polarization and prevents the light emitting to the downside (see the eigenmode in the inset of Figure 2a). According to the previous discussion, such a radiation pattern will lead to the efficient light absorption when the incident angle varies from $\phi = 0$ to $\phi = \pi$ (cf. eq 11). Due to the mode orthogonality of the even and the odd resonances, the incident-angle dependent absorption cross section of the wire-trough structure can be calculated by the temporal coupled-mode theory of eq 13. The results are shown as the black solid line in Figure 3b. We also use the numerical method to calculate the absorption cross section for

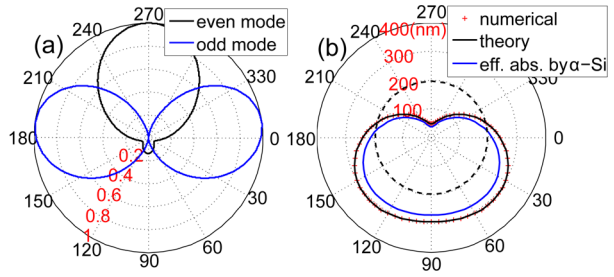

Figure 3. (a) Black and blue lines correspond to radiation pattern $|d(\theta)\rangle$ of the even and odd LMRs, respectively. (b) Black solid line and red cross line correspond to the incident-angle dependent absorption cross section of the wire-trough structure calculated by the temporal coupled-mode theory (eq 13) and the numerical method (FEM), respectively. The blue solid line represents the effective absorption cross section of the wire-trough structure after excluding the parasitic absorption by the metal trough. The black dashed line corresponds to the isotropic absorption cross section of the 110 nm diameter single nanowire calculated by FEM.

different incident angles (the cross line in Figure 3b). Indeed it shows an excellent agreement between the temporal coupled-mode theory and the numerical calculation.

Figure 3b illustrates that the wire-trough structure strongly enhances the broad-angle absorption cross section for one side (from $\phi = 0$ to $\phi = \pi$). To show the half-space absorption enhancement, we also plot the optimal single nanowire case, the absorption cross section of the 110 nm diameter single nanowire at the resonant frequency of the TM_{11} resonance in Figure 3b. We also calculate the effective absorption cross section after excluding the parasitic absorption by the metal trough (the blue solid line in Figure 3b). At the normal incident angle, the absorption cross section of the wire-trough structure shows 37% enhancement as compared with that of the single nanowire. Moreover, the enhancement covers a wide range of incident angle from $\phi = \pi/6$ to $\phi = 5\pi/6$, and the average enhancement is 39%.

Now we consider the half-space absorption enhancement in the case of TE polarization. Our simulation shows that the TE_{01} mode resonates at 664 nm. The far-field of the scattering field in the TE polarized case (Figure 4a) dominates in angles from $\theta = 7\pi/6$ to $\theta = 11\pi/6$. We also plot the incident-angle dependent absorption cross section of the wire-trough structure (the black solid line in Figure 4b). Indeed the dominant

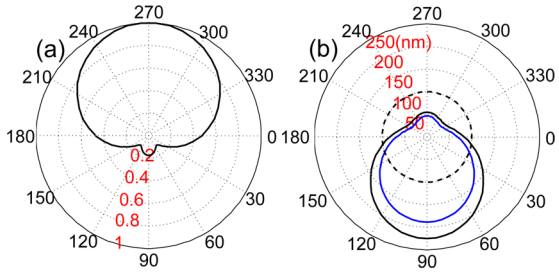

Figure 4. (a) Scattering field under the illumination of a 664 nm TE polarized wave. (b) The black solid line corresponds to absorption cross section of the wire-trough structure in TE polarized case. The blue solid line represents the effective absorption cross section of the wire-trough structure after excluding the parasitic absorption by the metal trough. The black dashed line corresponds to the isotropic absorption cross section of the 110 nm diameter single nanowire calculated by FEM.

DOI: 10.1021/acs.nanolett.5b02044
Nano Lett. 2015, 15, 5513−5518

absorptive angles have a π rotation from the far field, which agrees with the theoretical prediction. Compared with the optimal nanowire case (the dotted line in Figure 4b), the wire-trough structure exhibits strong absorption enhancement for the incident angle varying from $\phi = \pi/6$ to $\phi = 5\pi/6$. We also calculate the effective absorption by the embedded wire after excluding the parasitic absorption in the metal (the blue solid line in Figure 4b). At the normal incident angle, the absorption cross section of the embedded nanowire is enhanced 89% by the metallic trough structure.

Now let us show that half-space absorption enhancement can cover a broad wavelength range. We define the effective absorption as the integration of absorption cross section from $\phi = \pi/6$ to $\phi = 5\pi/6$. Figure 5 plots the effective absorption in the

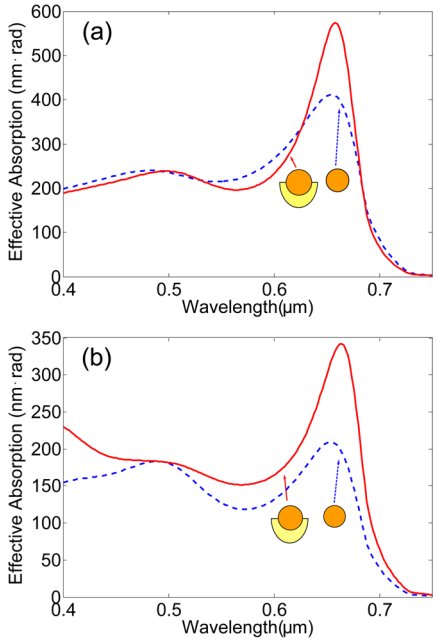

Figure 5. Effective half-space absorption cross section in the (a) TM polarized and (b) TE polarized cases. The red and blue lines correspond to the effective absorption cross section of the wire-trough structure and the optimal single nanowire, respectively.

wavelength ranging from 400 to 760 nm. For the TM polarized case (Figure 5a) the wire-trough structure shows 39% enhancement, and the average enhancement from 400 to 760 nm is 2% in comparison to the optimal single nanowire case. In the TE polarized case (Figure 5b), the wire-trough structure shows a broadband enhancement over the visible spectrum. At 664 nm, the wire-trough structure shows 64% enhancement, and the average enhancement from 400 to 760 nm is 26% as compared with the optimal single nanorod case.

In conclusion, we develop a framework for the half-space light absorption enhancement for leaky mode resonant nanowires. We show that nanowires with centrosymmetric geometry cross section have an upper limit under the half-space illumination. Based on the temporal coupled-mode equation, a reciprocity theory is developed for leaky mode resonances in order to connect the angle-dependent absorption cross section and the radiation pattern. To exceed the half-space limit it needs to break the centrosymmetry, and a desired radiation pattern should be noncentrosymmetric and dominate in the direction reciprocal to the illumination. We note that when the half-space light illuminates obliquely off the axis the developed reciprocity theory is still valid. In this case, the off-axial component needs to be taken into account when controlling the LMR radiation pattern.

We also numerically demonstrate the half-space absorption enhancement with a wire-trough structure. We show that the radiation pattern of the nanowire is strongly modified by the metallic trough and exhibits a desired profile for half-space absorption. As expected, at the resonant frequency, the trough structure enhances 39% and 64% for the TM and TE polarized cases in comparison to an optimal single nanowire. Moreover, the trough structure enables the enhancement over a broad wavelength range for both the TM and the TE polarizations. We note that it has been experimentally demonstrated that a metal troughs network is a remarkable transparent electrode with great mechanical flexibility.[33] Therefore, by combining the functionality of both absorption enhancement and transparent electrode, the trough structure is expected to augment the performance of applications including nanowire photodetectors, solar cells, and optical sensors.

AUTHOR INFORMATION

Corresponding Author

*E-mail: zhichao@zju.edu.cn.

Notes

The authors declare no competing financial interest.

ACKNOWLEDGMENTS

This work was financially supported by Fundamental Research Funds for the Central Universities (2014QNA3007). H.W. acknowledges the supports from National Basic Research of China (Grant No. 2013CB632702) and NSF of China (Grant No. 51302141). S.F. acknowledges the support of the U.S. Department of Energy (Grant No. DE-FG07ER46426).

REFERENCES

(1) Cao, L.; White, J. S.; Park, J.-S.; Schuller, J. A.; Clemens, B. M.; Brongersma, M. L. *Nat. Mater.* **2009**, *8*, 643.
(2) Cao, L.; Park, J.-S.; Fan, P.; Clemens, B.; Brongersma, M. L. *Nano Lett.* **2010**, *10*, 1229.
(3) Fan, P.; Chettiar, U. K.; Cao, L.; Afshinmanesh, F.; Engheta, N.; Brongersma, M. L. *Nat. Photonics* **2012**, *6*, 380.
(4) Brubaker, M. D.; Blanchard, P. T.; Schlager, J. B.; Sanders, A. W.; Roshko, A.; Duff, S. M.; Gray, J. M.; Bright, V. M.; Sanford, N. A.; Bertness, K. A. *Nano Lett.* **2013**, *13*, 374.
(5) Miao, J.; Hu, W.; Guo, N.; Lu, Z.; Zou, X.; Liao, L.; Shi, S.; Chen, P.; Fan, Z.; Ho, J. C.; Li, T.-X.; Chen, X. S.; Lu, W. *ACS Nano* **2014**, *8*, 3628.
(6) Liu, K.; Sakurai, M.; Liao, M.; Aono, M. *J. Phys. Chem. C* **2010**, *114*, 19835.
(7) Kind, H.; Yan, H.; Messer, B.; Law, M.; Yang, P. *Adv. Mater.* **2002**, *14*, 158.
(8) Hu, L.; Yan, J.; Liao, M.; Wu, L.; Fang, X. *Small* **2011**, *7*, 1012.
(9) Afsal, M.; Wang, C.-Y.; Chu, L.-W.; Ouyang, H.; Chen, L.-J. *J. Mater. Chem.* **2012**, *22*, 8420.
(10) Tang, L.; Kocabas, S. E.; Latif, S.; Okyay, A. K.; Ly-Gagnon, D.-S.; Saraswat, K. C.; Miller, D. A. *Nat. Photonics* **2008**, *2*, 226.
(11) Mann, S. A.; Garnett, E. C. *Nano Lett.* **2013**, *13*, 3173.
(12) Cao, L.; Fan, P.; Vasudev, A. P.; White, J. S.; Yu, Z.; Cai, W.; Schuller, J. A.; Fan, S.; Brongersma, M. L. *Nano Lett.* **2010**, *10*, 439.
(13) Brittman, S.; Gao, H.; Garnett, E. C.; Yang, P. *Nano Lett.* **2011**, *11*, 5189.
(14) Tian, B.; Zheng, X.; Kempa, T. J.; Fang, Y.; Yu, N.; Yu, G.; Huang, J.; Lieber, C. M. *Nature* **2007**, *449*, 885.
(15) Czaban, J. A.; Thompson, D. A.; LaPierre, R. R. *Nano Lett.* **2009**, *9*, 148.

DOI: 10.1021/acs.nanolett.5b02044
Nano Lett. 2015, 15, 5513−5518

(16) Dong, Y.; Tian, B.; Kempa, T. J.; Lieber, C. M. *Nano Lett.* **2009**, *9*, 2183.
(17) Tang, J.; Huo, Z.; Brittman, S.; Gao, H.; Yang, P. *Nat. Nanotechnol.* **2011**, *6*, 568.
(18) Varghese, O. K.; Paulose, M.; Grimes, C. A. *Nat. Nanotechnol.* **2009**, *4*, 592.
(19) Zhu, J.; Yu, Z.; Burkhard, G. F.; Hsu, C.-M.; Connor, S. T.; Xu, Y.; Wang, Q.; McGehee, M.; Fan, S.; Cui, Y. *Nano Lett.* **2009**, *9*, 279.
(20) Garnett, E.; Yang, P. *Nano Lett.* **2010**, *10*, 1082.
(21) Anttu, N.; Namazi, K. L.; Wu, P. M.; Yang, P.; Xu, H.; Xu, H.; Håkanson, U. *Nano Res.* **2012**, *5*, 863.
(22) Kim, S.-K.; Day, R. W.; Cahoon, J. F.; Kempa, T. J.; Song, K.-D.; Park, H.-G.; Lieber, C. M. *Nano Lett.* **2012**, *12*, 4971.
(23) Kim, C.-J.; Lee, H.-S.; Cho, Y.-J.; Kang, K.; Jo, M.-H. *Nano Lett.* **2010**, *10*, 2043.
(24) Dai, X.; Zhang, S.; Wang, Z.; Adamo, G.; Liu, H.; Huang, Y.; Couteau, C.; Soci, C. *Nano Lett.* **2014**, *14*, 2688.
(25) Persano, A.; Nabet, B.; Taurino, A.; Prete, P.; Lovergine, N.; Cola, A. *Appl. Phys. Lett.* **2011**, *98*, 153106.
(26) Hyun, J. K.; Lauhon, L. J. *Nano Lett.* **2011**, *11*, 2731.
(27) Wang, J.; Gudiksen, M. S.; Duan, X.; Cui, Y.; Lieber, C. M. *Science* **2001**, *293*, 1455.
(28) Wang, Z. L. *Mater. Sci. Eng., R* **2009**, *64*, 33.
(29) Ruan, Z.; Fan, S. *Phys. Rev. A: At., Mol., Opt. Phys.* **2012**, *85*, 043828.
(30) Fan, S.; Suh, W.; Joannopoulos, J. D. *J. Opt. Soc. Am. A* **2003**, *20*, 569−572.
(31) Hamam, R. E.; Karalis, A.; Joannopoulos, J. D.; Soljačić, M. *Phys. Rev. A: At., Mol., Opt. Phys.* **2007**, *75*, 053801.
(32) Ruan, Z.; Fan, S. *J. Phys. Chem. C* **2010**, *114*, 7324.
(33) Wu, H.; Kong, D.; Ruan, Z.; Hsu, P.-C.; Wang, S.; Yu, Z.; Carney, T. J.; Hu, L.; Fan, S.; Cui, Y. *Nat. Nanotechnol.* **2013**, *8*, 421.
(34) Palik, E. D. *Handbook of Optical Constants in Solids*; Academic Press: Boston, MA, 1991; Vol. *1*.

DOI: 10.1021/acs.nanolett.5b02044
Nano Lett. 2015, 15, 5513−5518